Kinetics and Rheology Characterization During Curing of Dicyanates

YUNG-TIN CHEN* and C. W. MACOSKO†

Department of Chemical Engineering and Materials Science, University of Minnesota, Minneapolis, Minnesota 55455

SYNOPSIS

Reaction kinetics and viscosity rise of a liquid dicyanate ester monomer, 1,1-bis(4-cyanatophenol)ethane, are characterized and fitted several models. Fourier transform infrared (FTIR) spectroscopy and differential scanning calorimetry (DSC) are used to obtain the isothermal reaction kinetic data. The liquid dicyanate resin shows second-order reaction kinetics in the early stage and approaches a plateau conversion at longer times with each curing temperature. Experimental data show that the diffusion limitation for dicyanate resin occurs well before the vitrification point. A two-step kinetic model and a Williams–Landel–Ferry- (WLF-) type diffusion-controlled kinetic model are developed to describe the entire range of curing. For the temperature range we studied (140°C–200°C), the WLF-type diffusion-controlled kinetic model gives a better prediction than the two-step kinetic model does. The viscosity rise during isothermal curing is characterized using disposable parallel plates. A Castro-Macosko type of equation is used to describe the isothermal viscosity rise. © 1996 John Wiley & Sons, Inc.

INTRODUCTION

Advanced composites made of cyanate resin/fiber reinforcements have found increased use in many areas due to their desirable properties. The principal uses for cyanate ester resins are (1) in the electronic market, because polycyanurate networks exhibit low dielectric loss characteristics, and (2) in composite materials for structural applications, because high glass transition temperatures are obtained as well as high fracture toughness and mechanical strength. A liquid dicyanate ester monomer, 1,1-bis(4-cyanatophenol)ethane, which has viscosity around 100 mPa s at room temperature, is ideal to achieve rapid on-line or in-mold fiber impregnation while not sacrificing characteristic matrix performance.[1-3]

The main reaction pathway of dicyanate ester is identified as the cyclotrimerization of dicyanate groups to form a highly crosslinked polytriazine network[4-11] (see Fig. 1). Trimerization rates of uncatalyzed dicyanates are slow and are a function of the concentration of active hydrogen impurities. This reaction is normally catalyzed by a mixture of transition metal cations and an active hydrogen initiator, such as nonylphenol. Curing behavior of dicyanate ester resins has been studied by several researchers.[7,8,10-12] They found that the reaction kinetics can be described by a simple second-order Arrhenius-type equation in the kinetic-controlled regime for the catalyzed systems. Osei-Owusu et al.[7] reported that the observed reaction rate showed a first-order dependence on the initial catalyst concentration. For the uncatalyzed system, the kinetics were described by a second-order autocatalytic model. Osei-Owusu and Martin[8] proposed a possible reaction scheme to describe the trimerization reaction, which consisted of four elementary reaction steps involving the monomer, the metal, and the cyanate/metal complexes. Their reaction scheme indicates that the trimerization reaction can be described by second-order kinetics with respect to monomer concentration and first-order kinetics in terms of catalyst concentration.

Reaction kinetics of cyanate ester reported by these researchers so far have all been in the kinetic-controlled regime. No attempt has been made to

* Present address: Polaroid Corp., 1265 Main Street, Building W4, Waltham, MA 02254.

† To whom correspondence should be addressed.

Journal of Applied Polymer Science, Vol. 62, 567–576 (1996)
 CCC 0021-8995/96/030567-10

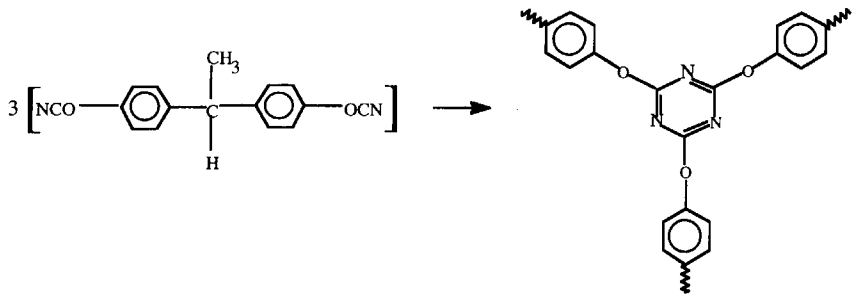

Figure 1 Polycyclotrimerization reaction of 1,1-bis(4-cyanatophenol)ethane to form triazine network.

model the entire curing behavior of cyanate ester resins, including the regime of diffusion control at higher conversion, as observed by Osei-Owusu et al.[7] and Chen and Macosko.[13] For curing high-performance resins such as cyanate and epoxy, it is important to have a working equation to describe the curing behavior near the regime of complete conversion. In this study, Fourier transform infrared (FTIR) spectroscopy and differential scanning calorimetry (DSC) are used to obtain the reaction kinetic data. A simple empirical model which takes into account the limiting conversion and a Williams–Landel–Ferry- (WLF-) type diffusion-controlled equation is used to describe the whole conversion range for the isothermal conversion measurement. The viscosity rise during isothermal curing is characterized using Rheometrics System IV and RMS-800 rheometers. A Castro-Macosko type of equation is used to describe the isothermal viscosity rise as a function of reaction conversion.

EXPERIMENTAL

Materials Used

The 1,1-bis(4-cyanatophenol)ethane was supplied by Rhone-Poulenc, Inc., under the trade name AroCy L-10. The catalyzed system consists of 100 parts by weight of 1,1-bis(4-cyanatophenol)ethane monomer and 2 parts by weight of nonylphenol (from Aldrich, Inc.) and 0.15 parts by weight of 8% zinc naphthenate (from Mooney Chemical, Inc.). The samples were prepared by first mixing the zinc naphthenate and nonylphenol in a 50-mL Pyrex glass bottle on a hot plate for 5 min (temperature about 80–90°C); this catalyst mixture was then mixed with the liquid dicyanate monomer at room temperature with a magnetic stir-bar for 3–5 min. After all the components were thoroughly blended, the mixture was placed in the refrigerator to retard any reaction that might occur at room temperature.

Conversion Characterization

DSC

DSC measurements were performed using a power-compensated Perkin-Elmer DSC-7 unit. Five to ten milligrams of samples were sealed in a stainless steel high-pressure pan (part number B018-2901). Caution was taken to assure good sealing of sample pans to prevent leaking. The sample pan was cured in the DSC oven at an isothermal temperature for different periods of time ranging from minutes to hours. The cured sample was quenched at 500°C/min to −70°C and then scanned from −70°C to 360°C at 10°C/min. The DSC scans yielded the glass transition temperature, T_g, and residual heat of reaction, ΔH_{res}. The temperature corresponding to the midpoint of the endothermic deflection of the baseline was taken as the T_g[14,15]; the residual heat of reaction was calculated from the exotherm area. The conversion of each sample was determined by dividing the residual heat of the sample by that of the uncured sample:

$$\alpha = \frac{\Delta H_{tot} - \Delta H_{res}}{\Delta H_{tot}} \quad (1)$$

where ΔH_{tot} is the total heat of reaction, which was determined to be 740 J/g at 10°C/min scan. This value was calculated from the exotherm area of an uncured sample divided by the mass of the sample. Three uncured samples were tested, and the average value was used as ΔH_{tot}. The accuracy of ΔH_{tot} is ±10 J/g. Shimp et al.[3] reported a value of 746 J/g for ΔH_{tot} for the same liquid dicyanate system. Osei-Owusu and Martin[7] reported the total heats of reaction at different heating rates for bisphenol A dicyanate (BADCy, trade name AroCy B-10). At 10°C/min, the ΔH_{tot} is 730 J/g.

FTIR Spectroscopy

FTIR measurements were performed with an IBM IR-44 spectrometer. Reactions were carried out in

situ with an in-house–designed temperature-controlled sample holder.[15] The isothermal curing temperature ranged from 125°C to 200°C. The spectrometer chamber was purged with nitrogen for approximately 20 to 30 min, and a background spectrum was collected. The sample in the holder was then put into position and the chamber was again purged for another 20 to 30 min. To start the reaction, the temperature was brought up to the setpoint quickly by setting the initial transformer voltage at 120 V for 20 to 30 s. The time for the heater to reach the set temperature was about 20 s. After this initial time, the voltage was returned to 30 V for the remainder of the experiment. A spectrum was taken every 1 or 2 min at 15 scans with resolution of 2 cm^{-1}. By monitoring the spectra as time proceeded, the changes in the area of the reactant peak could be evaluated. The experiment was completed when the reactant peaks showed little or no change. Fractional conversion of dicyanate ester was calculated from the peak area of the dicyanate vibration at 2270 cm^{-1} normalized by the C—H stretch at 2950 cm^{-1}.[9,15] Assuming that the peak areas are directly proportional to the concentration, the conversion of dicyanate functional group at different times can be calculated as[7]

$$\alpha(t) = 1 - \frac{I(t)_{2270}/I(0)_{2270}}{I(t)_{2950}/I(0)_{2950}} \quad (2)$$

where $I(t)_{2270}$ is the absorbance intensity at 2270 at time t; $I(t)_{2950}$ is the absorbance intensity at 2950 at time t; $I(0)$ is the initial absorbance intensity; and $\alpha(t)$ is the fractional conversion of dicyanate functional groups.

Viscosity Characterization

Viscosity measurements were performed using Rheometrics System IV and RMS-800 rheometers. Steady shear viscosity measurements were made using modified 50-mm-diameter disposable aluminum parallel plates. The disposable plate was glued to an aluminum cup with high-temperature silicone adhesives. The disposable plates were preheated in the rheometer environmental chamber for approximately 5 min at a preset temperature. The gap between the plates was zeroed at that temperature. The plates were then separated quickly, and the prepared samples were rapidly injected between the plates with a syringe. The plates were then brought back together to a gap of approximately 1.5 mm. The environmental chamber was closed and purged with nitrogen gas. Loading of the sample was done as quickly as possible to minimize the heat loss. The temperature was then brought back to the preset temperature in less than a minute.

The temperature-dependent viscosities were measured by a Schott Gerate capillary viscosimeter in a silicone oil bath at different temperatures. The working viscosity range of the tube is between 1 and 300 cP, and the typical flow time between the markers is about 200 s. A pure liquid dicyanate resin without a catalyst was used for this measurement. Viscosity measurements up to 150°C were obtained. Beyond this temperature, the experiment was not pursued for safety reasons.

RESULTS AND DISCUSSION

Conversion Data from FTIR and DSC

The normalized conversion data from FTIR at 140, 150, 160, 165, 180, and 200°C are shown in Figure 2. The conversion reached a plateau value at the end of curing for each temperature. The conversion data from DSC measurements at 165, 180, and 200°C are shown in Figure 3. The reproducibility of the DSC technique is shown at 165°C. The conversions from FTIR and DSC measurements all agree within ±5%; however, within this range the FTIR values are consistently higher. A comparison of DSC and FTIR conversion measurements is shown in Figure 4. DSC is convenient for characterizing thermosets. Its ability to obtain glass transition temperature, T_g,

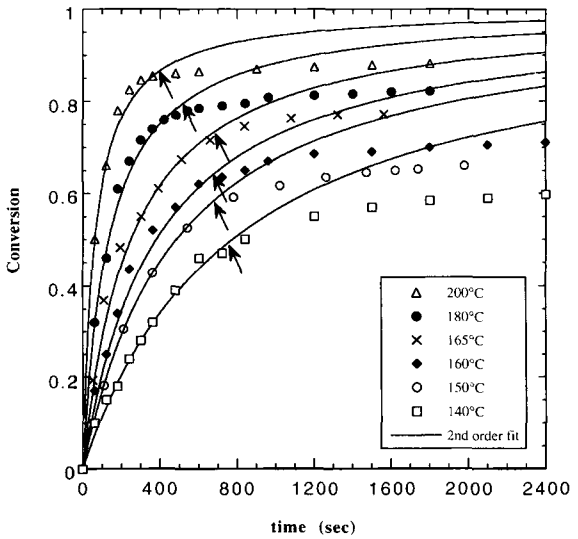

Figure 2 Experimental conversion versus curing time of 1,1-bis(4-cyanatophenol)ethane from FTIR measurements. Arrows are the deviation points from second-order kinetic fit.

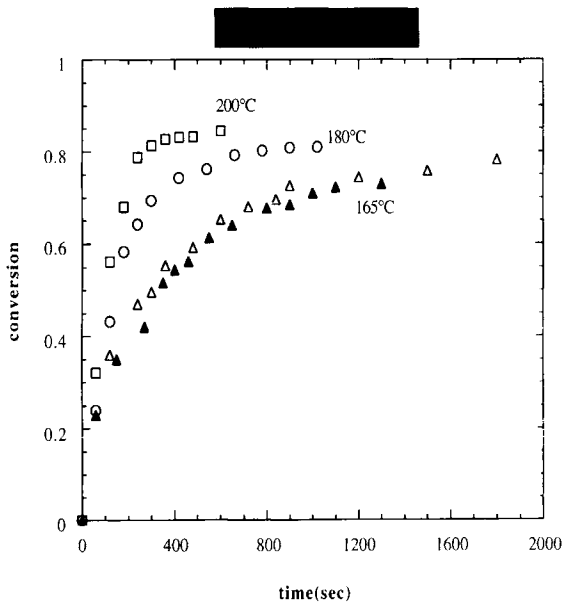

Figure 3 Experimental conversion versus curing time of 1,1-bis(4-cyanatophenol)ethane from DSC measurements. Reproducibility is shown at 165°C.

and heat of reaction, ΔH, at the same time when measuring reaction conversion is one reason that it is so popular. The major advantage of FTIR is its fast speed of obtaining kinetic data. The whole isothermal kinetic curve can be obtained in one continuous experiment.

Kinetic Models and Parameter Determination

Two-Step Plateau Kinetic Model

In this section, we will use different kinetic models to describe the conversion data of the liquid dicyanate system, L-10. Because the experimental data from FTIR measurements are more complete, we will use these data for kinetic modeling. As indicated in Figure 2, the rate of dicyanate conversion is initially rapid and then slows down, reaching a plateau conversion. The extent of conversion at which the reaction becomes dominated by mass transfer was dependent on the curing temperature. It was observed in our experiments and also indicated by Simon et al.[12] that the onset of diffusion control occurred well before vitrification. As shown in Figure 2, the onset of diffusion control increases with increasing temperatures, as does the maximum or plateau conversion. For example, the plateau conversion is about 78% at 165°C after 1 h of curing.

The conversion data prior to the plateau can be fitted to a second-order kinetics equation used by Osei-Owusu et al.[7,8] and Gupta and Macosko.[10,11] The incomplete reaction obtained during isothermal processes has been explained in terms of diffusion-controlled effects for several epoxy systems. When the increasing T_g approaches the isothermal curing temperature, the molecular mobility is strongly reduced and the reaction becomes diffusion-controlled and eventually stops.[16] It is possible to incorporate the diffusion-controlled effect into the kinetics equation by modifying the rate constants. Batch,[14] Wisanrakkit and Gillham,[17] and Chern and Poehlein[18] relate changes in free volume to changes in the reaction rate constants with conversion, adopting a semiempirical equation for variation of the reaction rate constants. On the other hand, it is also possible to modify empirically the simple *n*th-order kinetics equation by assuming the reaction rate drops to zero at a plateau conversion.[19] The plateau conversion can be empirically expressed as follows:

$$\alpha_p = a + bT_{\text{cure}} \tag{3}$$

where α_p is the plateau conversion and the fitted parameters a and b can be obtained by the linear regression of Figure 5 [a = 0.0533 and b = 0.0042 $(°C)^{-1}$, respectively]. According to this linear relationship between curing temperature and plateau conversion, the polymerization reaction will be complete when the curing temperature reaches 225.4°C.

The isothermal curing behavior shown in Figure 2, having a zero reaction rate at the later curing stage, can be modeled by a two-step rate equation:

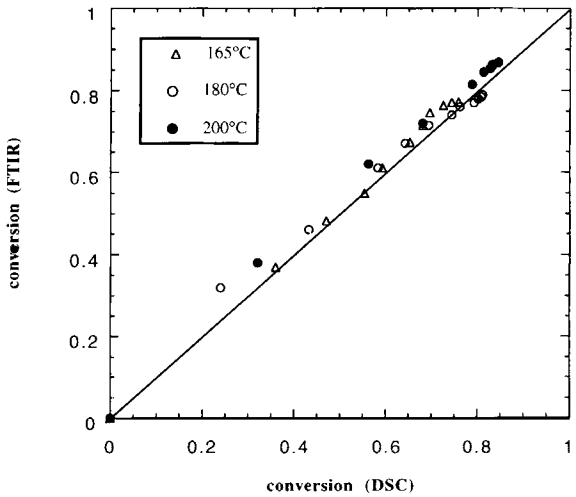

Figure 4 Comparison of DSC and FTIR conversion measurements of 1,1-bis(4-cyanatophenol)ethane.

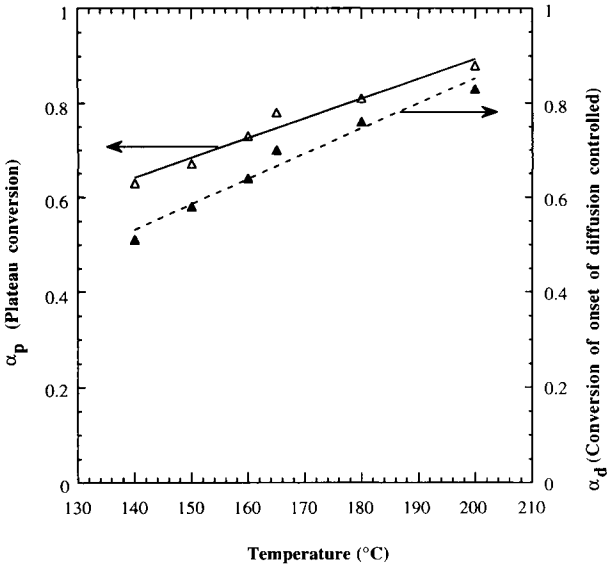

Figure 5 Plateau conversion and conversion of onset of diffusion-controlled versus curing temperature for liquid dicyanate resin. Solid line is the linear model fit (eqs. 3 and 5).

$$\frac{d\alpha}{dt} = k_1(1 - \alpha)^{n_1};\ \alpha < \alpha_d$$

$$\frac{d\alpha}{dt} = k_2(\alpha_p - \alpha)^{n_2};\ \alpha \geq \alpha_d \qquad (4)$$

where α_d is the onset of diffusion control and n_1, n_2 are the reaction kinetic exponents. The onset of diffusion control, α_d, increased with increasing curing temperatures, as indicated in Figure 2. It can be obtained by locating the point where the experimental data starts to deviate from the second-order kinetic model. The relationship between α_d and curing temperature is plotted in Figure 5. A linear relationship between α_d and curing temperature is observed from this plot:

$$\alpha_d = c + dT_{\text{cure}} \qquad (5)$$

The slope, d, and intercept, c, obtained from Figure 5 are 0.0053 $(°C)^{-1}$ and −0.1995, respectively. This means that there will be no diffusion-controlled effect when the curing temperature reaches 226°C.

The Arrhenius rate constants, $k_i = A_i \exp(-E_i/RT)$, can be determined by the best fit from Figure 6. The rate constant, k_1, is obtained by fitting the initial conversion data versus time, assuming the second-order reaction. Once k_1 is obtained, α_d can be determined by comparing the deviation point from the second-order kinetic fit. The k_2 and n_2 can then be evaluated by fitting the reaction rate versus conversion after α_d by multiple regression techniques. The kinetic parameters obtained are listed in Table I.

WLF Diffusion-Controlled Model.

A more rigorous treatment of a diffusion-affected polymerization reaction was also investigated. Gillham and coworkers[16,17] developed a diffusion-controlled kinetic model:

$$\frac{1}{k(\alpha, T)} = \frac{1}{k_T(T)} + \frac{1}{k_D(\alpha, T)} \qquad (6)$$

where k is the overall rate constant, k_T is the true rate constant (Arrhenius), and k_D is the diffusion rate constant. The argument is that the time scale for the overall reaction is a sum of the time for diffusion of reactants and the time for the polymerization reaction. The preceding equation shows that the overall rate constant is governed at one extreme by the Arrhenius rate constant when $k_T \ll k_D$ (prior to vitrification), and at the other extreme by the diffusion rate constant when $k_D \ll k_T$ (after vitrification).

The diffusion rate constant can be expected to be inversely proportional to the relaxation time of the polymer segments. This suggests that the temperature dependence of k_D can be described by the well-known WLF equation[16]:

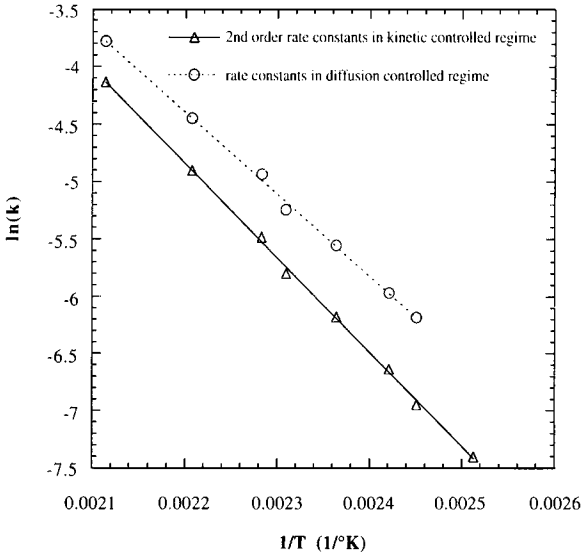

Figure 6 Arrhenius plot of the rate constants in kinetic-controlled regime and diffusion-controlled regime as a function of $1/T$.

$$\log \frac{k_D(T)}{k_D(T_g)} = \frac{C_1(T - T_g)}{C_2 + |T - T_g|} \tag{7}$$

where C_1 and C_2 are fitting parameters, and $k_D(T_g)$ is assumed constant. Once the correlation between glass transition temperature, T_g, and conversion can be established, the diffusion rate constant, k_D, can be expressed explicitly as a function of temperature and conversion. To apply this WLF-type equation to a diffusion-controlled kinetic model, it is essential to establish a relationship between the glass transition temperature, T_g, and the conversion. The glass transition temperature of 1,1-bis(4-cyanatophenol)ethane as a function of conversion is given in Figure 7. The glass transition temperatures were fitted with an empirical equation derived by Havlicek and Dusek[20]:

$$\frac{1}{T_g} = \frac{(1 - \alpha)}{T_{g0}} + \frac{\alpha}{T_{g\infty}} + C\alpha(1 - \alpha) \tag{8}$$

where α is the conversion, T_{g0} is the glass transition temperature of the unreacted polymer, which is equal to 193.1K determined by the best fit of the experimental data, $T_{g\infty}$ is the glass transition of the fully cured polymer, and C is an adjustable parameter determined as 5.6×10^{-4}. $T_{g\infty}$ was taken as 494.3K, determined by rescanning the fully cured sample.

The overall rate constant, k, is obtained by the experimental values, α, and $d\alpha/dt$:

$$k = \frac{d\alpha/dt}{(1 - \alpha)^2} \tag{9}$$

The Arrhenius rate constant, k_T, is obtained by fitting the second-order rate equation before α_d. The diffusion rate constant, k_D, follows directly from eq. (6):

$$\frac{1}{k_D} = \frac{1}{k} - \frac{1}{k_T} \tag{10}$$

The experimental overall rate constant as a function of conversion is shown in Figure 8 at an isothermal curing temperature of 165°C.

The general expression of the diffusion rate constant following the WLF model can be described empirically as[21]

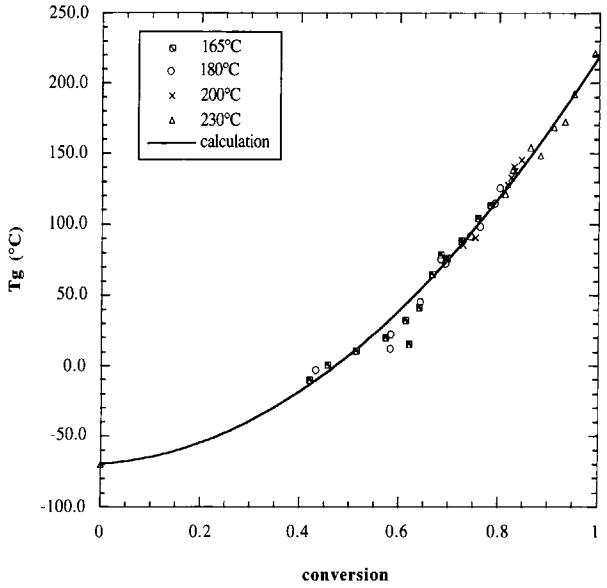

Figure 7 Glass transition temperature of 1,1-bis(4-cyanatophenol)ethane as a function of conversion. Solid line is calculated from eq. 8.

Table I Model Parameters of Kinetic Constants for Liquid Dicyanate Resins

Two-Step Plateau Kinetic Model [Eqs. 3–5)]		
$A_1 = 587720\ (s^{-1})$	$E_1 = 68500$ (J/mol)	$n_1 = 2$
$A_2 = 81060\ (s^{-1})$	$E_2 = 59320$ (J/mol)	$n_2 = 1.32$
$a = 0.0533$	$b = 0.0042\ (°C^{-1})$	
$c = -0.1995$	$d = 0.0053\ (°C^{-1})$	

WLF Diffusion-Controlled Model [Eqs. (8–12)]		
$A = 587720\ (s^{-1})$	$E = 68500$ (J/mol)	$n = 2$
$T_{g0} = 193.1K$	$C = 5.6 \times 10^{-4}$	$k_{D0} = 0.024\ (s^{-1})$
$C_1 = 7.1\ (K^{-1})$	$C_2 = 51.6$ (K)	$D = 275 - 1.03\ T_{cure}$ (K)

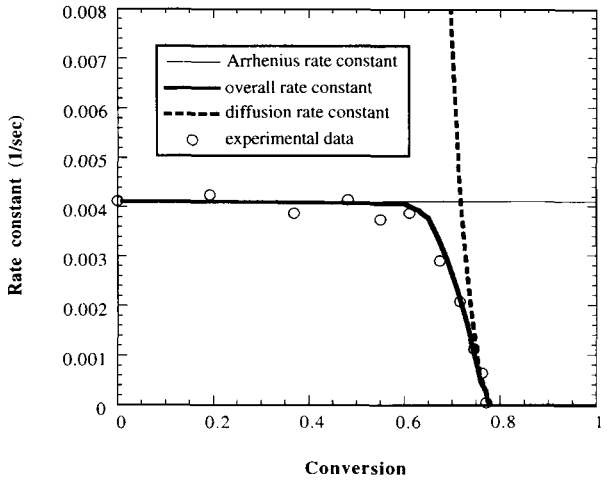

Figure 8 Experimental and predicted rate (Arrhenius, diffusion, and overall) constants versus conversion at 165°C for liquid dicyanate system.

$$\log \frac{k_D}{k_{D0}} = \frac{C_1(T_c - T_g - D)}{C_2 + |T_c - T_g - D|} \tag{11}$$

where k_{D0} is an adjustable parameter. Parameter D employed in this equation takes into account the difference between the curing temperature, T_c, and the glass transition temperature, T_g, at the onset of diffusion control point. As shown in Figure 9, for the liquid dicyanate ester, the glass transition temperature at the onset of the diffusion control point is much lower than the curing temperature. The difference D, however, is decreased with increasing curing temperature and can be readily obtained from experiments. The relationship between D and curing temperature can be expressed by the following empirical relationship:

$$D = 274.5 - 1.03T_c \tag{12}$$

It was suggested by Wisanrakkit and Gillham[17] that the WLF universal constant, 51.6, could be used for the fitting constant, C_2. With the parameters D and C_2 known, the plot of the natural logarithm of diffusion rate constant, k_D, versus $(T_c - T_g - D)/(51.6 + |T_c - T_g - D|)$ will give the values of k_{D0} and C_1. The values of k_{D0} and C_1 obtained are 0.024 (1/s) and 7.1 (1/°K), respectively.

The calculated diffusion control rate constant, Arrhenius rate constant, and overall rate constant at a curing temperature of 165°C are plotted in Figure 8 as a function of conversion. The comparison between the experimental and calculated overall rate constant is also shown. The WLF diffusion-controlled model adequately predicts the rate constants.

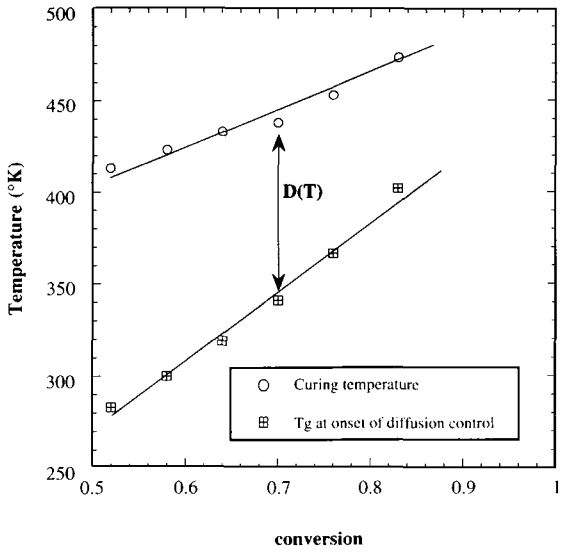

Figure 9 Glass transition temperature at onset of diffusion control and curing temperature of 1,1-bis(4-cyanatophenol)ethane as a function of conversion.

As a result, the diffusion-controlled kinetic model describes the curing behavior well for the liquid dicyanate ester system, as shown in Figure 10. Excellent agreement between experimental conversion as a function of curing time and model calculation is obtained. The calculations from the two-step plateau model are also plotted in the same graph for comparison. For curing temperature at 165°C, the two-step plateau model predicts lower conversion than

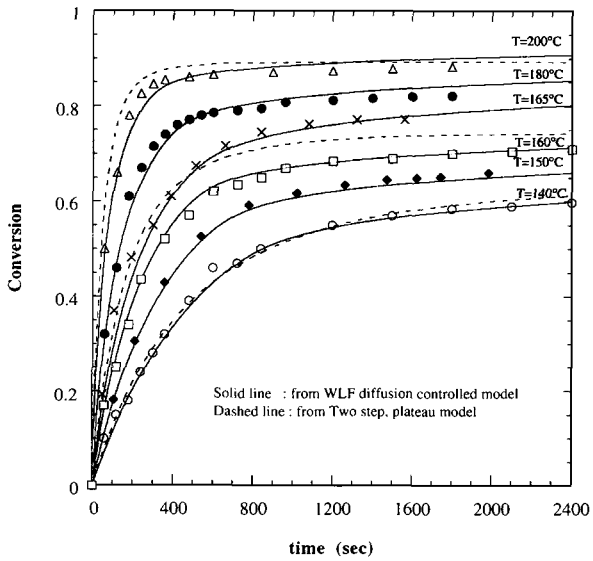

Figure 10 Comparison of experimental data vs. WLF diffusion-controlled and two step, plateau model predictions of 1,1-bis(4-cyanatophenol)ethane. (Two-step plateau-model fits are only shown with 140, 165, and 200°C.)

experimental data because the model is very sensitive to the plateau conversion, α_p. The deviation between the linear fit and the experimental α_p, as shown in Figure 5, at curing temperature of 165°C explains the discrepancy in Figure 10. The comparison in Figure 10 suggests that the WLF diffusion-controlled model is better than the two-step plateau model.

Chemorheology Model.

The effect of temperature dependence on viscosity is fitted to an Arrhenius temperature-dependent viscosity function based on the temperature dependence of the initial viscosity:

$$\eta(cP) = 3.32 \times 10^{-6}\exp\left(\frac{42903}{RT}\right) \tag{13}$$

Steady shear viscosity as a function of time for three different isothermal measurements at 140°C, 150°C, and 160°C is shown in Figure 11. The same experiments were repeated twice and, as shown, good reproducibility was obtained. The temperature control of the rheometer oven is within ±1°C.

Modeling of the reactive mold filling requires an expression that relates the viscosity to process conditions and the state of polymerization. In general, viscosity is a function of temperature, conversion, and shear rate:

$$\eta = \eta(T, \alpha, \dot{\gamma}) \tag{14}$$

Temperature influences viscosity in two opposing ways. Raising the temperature will cause viscosity to drop at a given conversion but will increase the reaction rate, causing an increase in conversion and viscosity. To separate these effects, viscosity should be explicitly related to reactive group conversion. The variation of viscosity and extent of reaction must be monitored at the same temperature. Castro and Macosko[22,23] have followed such an approach to obtain the following empirical relation:

$$\eta = A_\eta\exp\left(\frac{E_\eta}{RT}\right)\left[\frac{\alpha_g}{\alpha_g - \alpha}\right]^{A+B\alpha} \tag{15}$$

where α is the conversion, α_g is the conversion at gel point, and A_η, E_η, A, and B are constants. This equation adequately predicts divergence of the viscosity at the gel point.

As for the shear rate dependency, Macosko and coworkers[24-29] have found experimentally that the viscosity for several polyurethane systems is independent of the rate of shearing up to at least 100 Pa s. Therefore, because the proposed study is targeted for a low-viscosity process, the shear dependency of viscosity will be neglected.

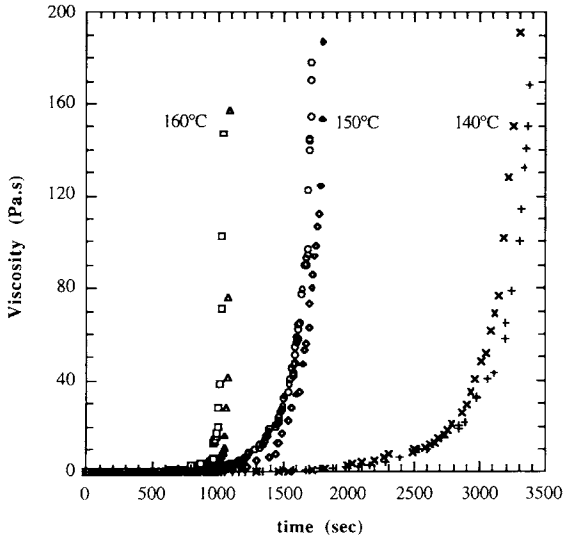

Figure 11 Viscosity rise of liquid dicyanate resin as a function of time at 140, 150, and 160°C.

To obtain the rheokinetic relationship, the variation of viscosity and extent of reaction were monitored at the same temperature. The extent of reaction was obtained at the same temperature using FTIR. By taking isochrones of viscosity and extent of reaction, a viscosity-conversion correlation was constructed. Repeating the procedure at different temperatures allowed the variation with temperature to be included in the correlation. The reduced viscosity-conversion plot of the liquid dicyanate resin is illustrated in Figure 12. The reduced viscosity is defined as

$$\eta_{\text{red}} = \frac{\eta}{\eta_0} \tag{16}$$

where η_0 is the initial viscosity using eq. (13). A good correlation between experimental data and model prediction was obtained. The fact that an exponential temperature dependence [Eq. (13)] works well is probably due to the fact that $T_g < 50$°C over the entire pre-gel range. The fitted parameters based on the Castro-Macosko equation [eq. (15)] is tabulated in Table II. The gel conversion is 0.64 ± 0.02. Similar conversions were found by dynamic mechanical measurements. These gel conversions are in agreement with Gupta[11] and Osei-Ourisu[7,8] for curing of 2,2-bis(4-cyanatophenol)propane, but higher than reported by Bauer and coworkers.[4-6]

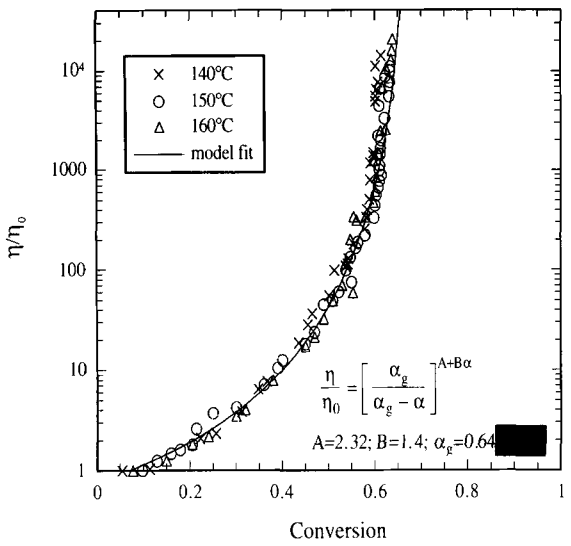

Figure 12 Reduced viscosity rise as a function of conversion for liquid dicyanate resin. Solid line is the model fitting using the Castro–Macosko equation.

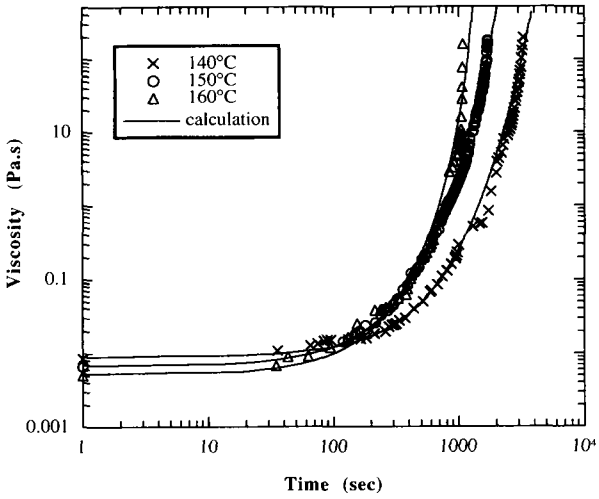

Figure 13 Plots of viscosity rise vs. time, comparisons between model predictions (eqs. 13 and 15) and experimental data.

Using the kinetic models obtained previously, one can construct a viscosity–time relationship. The experimental data and model prediction based on the WLF diffusion-controlled kinetic model of viscosity–time relation are reproduced in Figure 13. At lower temperatures, the viscosities are higher initially but rise more slowly due to the slower reaction rate. At early stages of the reaction, the viscosity is mainly affected by the temperature.

CONCLUSION

The kinetic studies of the liquid dicyanate ester, 1,1-bis(4-cyanatophenol)ethane, indicate that the monomer follows second-order reaction kinetics in the kinetic-controlled regime and approaches a plateau conversion at a certain curing temperature, which is less than complete conversion. It is found that the diffusion limitation for dicyanate resin occurs well before the vitrification point. This phenomenon is very different from the case of an epoxy system. A two-step kinetic model with the addition of a plateau conversion in the diffusion-controlled regime is developed to describe the entire curing curve. Another more rigorous WLF-type diffusion-controlled kinetic model is also examined. Both kinetic models predict the experimental data reasonably well. For the temperature range we studied (140–200°C), a WLF-type diffusion-controlled kinetic model gives a better prediction than the two-step kinetic model does. The fact that diffusion-controlled kinetics occur well before vitrification for the cyanate ester resin is of great interest. Further study in relating the cyanate cyclotrimerization to this early diffusion limitation phenomenon should be investigated. For viscosity characterization, a Castro–Macosko-type equation was formed to describe the isothermal viscosity rise of 1,1-bis(4-cyanatophenol)ethane.

Table II Model Parameters Obtained from the Isothermal Viscosity Characterization of the Catalyzed Liquid Dicyanate Resin

A_η (Pa s)	E_η (J/mol)	A	B	α_g
3.32×10^{-8}	42903.5	2.32	1.4	0.64 ± 0.02

This work is financially supported by the Center for Interfacial Engineering at the University of Minnesota and Ciba-Geigy Corporation. The authors would like to thank David Shimp of Ciba-Geigy for providing the reactants and for numerous helpful discussions and Leo Kasehagen of the University for helpful comments on the manuscript.

REFERENCES

1. D. A. Shimp, *Proc. ACS Div. Polym. Mater. Sci. Eng.*, **54**, 107 (1986).
2. D. A. Shimp and W. M. Craig, Jr., 34th International SAMPE Symposium, Reno, May 8–11, 1326 (1989).
3. D. A. Shimp, J. R. Christenson, and S. J. Ising, Rhone-Poulenc Publication (1991).

4. M. Bauer, J. Bauer, and G. Kuhn, *Acta Polymerica,* **37,** 11 (1986).
5. J. Bauer, M. Bauer, R. Ruhmann, and G. Kuhn, *Acta Polymerica,* **40**(6), 379 (1989).
6. J. Bauer, P. Lang, W. Burchard, and M. Bauer, *Macromolecules,* **24**(9), 2634 (1991).
7. A. Osei-Owusu, G. C. Martin, and J. T. Gotro, *Polym. Eng. Sci.,* **32,** 1604 (1991).
8. A. Osei-Owusu and G. C. Martin, *Polym. Eng. Sci.,* **31,** 1604 (1992).
9. A. Gupta, Ph.D. thesis, University of Minnesota, December 1991.
10. A. Gupta and C. W. Macosko, *Makromol. Chem. Macromol. Symp.,* **45,** 105 (1991).
11. A. Gupta and C. W. Macosko, *Macromolecules,* **26,** 2455 (1993).
12. S. L. Simon, J. K. Gillham, and D. A. Shimp, *Proc. ACS Div. Polym. Matls. Sci. & Eng.,* **62,** 96 (1990).
13. Y. T. Chen and C. W. Macosko, 24th International SAMPE Technical Conference, October 20–22, T630 (1992).
14. G. L. Batch, Ph.D. dissertation, University of Minnesota, 1989.
15. Y. T. Chen, Ph.D. dissertation, University of Minnesota, 1993.
16. J. K. Gillham, *Polym. Eng. Sci.,* **26,** 1429 (1986).
17. G. Wisanrakkit and J. K. Gillham, *Journal of Coatings Technology,* **62**(783), 35 (1990).
18. C. S. Chern and G. W. Poehlien, *Polym. Eng. Sci.,* **27,** 788 (1991).
19. J. M. Kenny and A. Trivisano, *Polym. Eng. Sci.,* **31,** 1426 (1991).
20. I. Havlicek and K. Dusek, in *Crosslinked Epoxies,* B. Sedlacek and J. Kahovec Eds., Walter de Gruyter & Co., Berlin, 1987, p. 417.
21. D. H. Kim and S. C. Kim, *Polym. Eng. Sci.,* **29,** 456 (1989).
22. J. M. Castro and C. W. Macosko, *Soc. Plast. Eng. Tech. Papers,* **26,** 434 (1980).
23. J. M. Castro and C. W. Macosko, *AIChE J.,* **25,** 89 (1982).
24. C. W. Macosko, in *Fundamentals of Reaction Injection Molding,* Chap. 2, Hanser Publishers, New York, 1989.
25. S. D. Lipshitz and C. W. Macosko, *J. Appl. Polym. Sci.,* **21,** 2029 (1977).
26. E. B. Richter and C. W. Macosko, *Polym. Eng. Sci.,* **18,** 1012 (1978).
27. V. M. Gonzalez-Romero and C. W. Macosko, *ACS Org. Coat. & Appl. Polym. Sci. Preprints,* **48,** 934 (1983).
28. V. M. Gonzalez-Romero and C. W. Macosko, *Polym. Process Eng.,* **3,** 173 (1985).
29. R. E. Camargo, V. M. Gonzalez, C. W. Macosko, and M. Tirrell, *Rubber Chem. Tech.,* **56,** 38 (1983).

Received January 5, 1995
Accepted December 11, 1996